

Negative Differential Conductance and Hot Phonons in Suspended Nanotube Molecular Wires

Eric Pop,^{†1,2} David Mann,^{†1} Jien Cao,^{†1} Qian Wang,¹ Kenneth Goodson² and Hongjie Dai^{1,*}

¹ *Department of Chemistry and Laboratory for Advanced Materials, Stanford University, Stanford, CA 94305, USA*

² *Department of Mechanical Engineering and Thermal Sciences, Stanford University, Stanford, CA 94305, USA*

Freely suspended single-walled carbon nanotubes (SWNTs) exhibit reduced current carrying ability compared to those lying on substrates, and striking negative differential conductance (NDC) at low electric fields. Theoretical analysis reveals significant self-heating effects including electron scattering by hot non-equilibrium optical phonons. Electron transport characteristics under strong self-heating are exploited for the first time to probe the thermal conductivity of individual SWNTs ($\sim 3600 \text{ Wm}^{-1}\text{K}^{-1}$ at $T=300 \text{ K}$) up to $\sim 700 \text{ K}$, and reveal a $1/T$ dependence expected for Umklapp phonon scattering at high temperatures.

* E-mail: hdai@stanford.edu

[†] *These authors contributed equally.*

The current carrying ability of materials is fundamental and important to a wide range of applications from power transmission to high performance electronics. It is now well established that when in contact with a substrate, metallic SWNTs can carry tens of micro-amperes of current.¹⁻² Nevertheless, little is known about the high bias transport properties of suspended SWNTs in native unperturbed states. In general, high field transport in quasi 1D materials is significantly affected by the surrounding environment due to reduced dimensionality for thermal conduction and phonon transport. The latter will be important to high power and speed applications of 1D materials, and neither has been fully explored.

Here, we uncover that suspended SWNTs display drastically different electron transport and phonon scattering than those on substrates. Experimentally, suspended ($L=0.6$ to $10\text{ }\mu\text{m}$ long) SWNTs with Pt electrical contacts were obtained by direct growth across pre-formed trenches (Fig.1), as described previously.^{3,4} Devices comprised of an individual nanotube with a non-suspended (lying on silicon nitride) and a suspended segment over a trench were also fabricated (Fig. 1a and 1b) for comparison. The devices were characterized by atomic force microscopy (AFM) and scanning electron microscopy (SEM) to obtain nanotube diameter (d) and length (L) information. All electrical measurements were carried out in *vacuum* at *room temperature* (R.T., $T_0\sim 300\text{ K}$).

The same-length suspended and non-suspended portions of a metallic SWNT ($d\sim 2.4\text{ nm}$, $L\sim 3\text{ }\mu\text{m}$, Fig. 2) exhibit drastically different current vs. voltage (I - V) characteristics in the high bias regime (Fig. 2a). The non-suspended nanotube portion shows monotonic I - V with I approaching $\sim 20\text{ }\mu\text{A}$ under increasing V , while the current in the suspended tube reaches a peak of $I_{peak}\sim 5\text{ }\mu\text{A}$ followed by a pronounced NDC (Fig. 2a).

We find that current peaking and NDC are universal transport properties of all suspended SWNTs with lengths in the range of 0.6-10 μm (Fig. 3a). A systematic decrease in I_{peak} is seen for longer suspended tubes with $I_{peak} \sim 12 \mu\text{A}/L$ (with L in μm) measured with > 30 suspended tubes (Fig. 3b).

The NDC behavior of freely suspended SWNTs starting at electric fields as low as 200 V/cm (for $L \sim 10 \mu\text{m}$ tubes) cannot be explained by the velocity saturation expected theoretically at much higher fields ($\sim 5 \text{ kV/cm}$) under isothermal conditions.^{5,6} Isothermal conditions (i.e., no appreciable self-heating) are typically assumed for electron transport in SWNTs on substrates due to heat sinking by the substrate.¹⁻⁷ The I - V curve can be calculated by $I = V/R(V)$ with resistance $R(V) = R_c + (h/4q^2)[L + \lambda_{eff}^{RT}(V)]/\lambda_{eff}^{RT}(V)$ where R_c is the contact resistance. The R.T. total electron scattering mean free path⁸ (mfp) is $\lambda_{eff}^{RT}(V) = [1/\lambda_{ac}^{RT} + 1/\lambda_{op,em}^{RT}(V)]^{-1}$ with an acoustic phonon (AC) scattering mfp ^{9,10} $\lambda_{ac}^{RT} \sim 1600 \text{ nm}$ and optical phonon (OP) emission mfp $\lambda_{op,em}^{RT}(V) = \hbar\omega_{op}L/qV + \lambda_{op,min}$,⁷ where the first term (q = electron charge) represents the distance required by electrons to reach the optical phonon emission threshold¹ energy $\hbar\omega_{op} \sim 0.18 \text{ V}$, and $\lambda_{op,min} \sim 15 \text{ nm}$ ^{1,9} is the mfp of OP emission after reaching the threshold. At R.T., scattering by OP absorption can be neglected due to the large energy of optical phonons in SWNTs ($\hbar\omega_{op} \gg k_B T$) and their low population. The I - V characteristic thus calculated fits well the experimental data of the SWNT on substrate for $V < \sim 1 \text{ V}$ (Fig. 2a). The model calculation over-estimates currents for $V > \sim 1 \text{ V}$ (Fig. 2a), indicating that the isothermal condition may not hold for $V > \sim 1 \text{ V}$ under which self-heating starts to manifest in the $L \sim 3 \mu\text{m}$ SWNT on substrate.

For suspended SWNTs in vacuum, when heat dissipation only occurs along the tube length to the contacts (1D thermal transport), we consider self-heating and a bias-dependent temperature profile of the nanotube. The I - V characteristics are calculated by $I=V/R(V,T)$, where $R(V,T) = R_c + (h/4q^2)[L + \lambda_{eff}(V,T)]/\lambda_{eff}(V,T)$ and $\lambda_{eff}(V,T) = (1/\lambda_{ac}(T) + 1/\lambda_{op,ems}(V,T) + 1/\lambda_{op,abs}(V,T))^{-1}$ are V and in turn T dependent. The AC scattering mfp scales with T as $\lambda_{ac}(T) = \lambda_{ac}^{RT}(300K/T)$ since acoustic phonons are thermally occupied at energies $\hbar\omega_{ac} < k_B T$ at R.T. and above. The OP emission and absorption mfp are $\lambda_{op,ems}(T) = \hbar\omega_{op} L / qV + \lambda_{op,min}[N_{op}(300K) + 1]/[N_{op}(T) + 1]$ and $\lambda_{op,abs}(T) = \lambda_{op,min}[N_{op}(300K) + 1]/N_{op}(T)$ respectively, with $N_{op} = 1/[\exp(\hbar\omega_{op}/k_B T) - 1]$ as the OP occupation number. In the limit of $N_{op} \sim 0$ (below or near R.T. for $\hbar\omega_{op} > k_B T$) this model gives a long OP absorption mfp , $\lambda_{op,abs}(T)$, as expected.

Under a given bias V the lattice temperature of the suspended SWNT is determined by the power dissipation $P=I^2(R - R_c)$ and thermal conductivity $\kappa(T)$ of the tube. The average temperature along the tube is $T = T_0 + I^2(R - R_c)L/(12\kappa(T)A)$ where $T_0 \sim 300$ K is the electrode temperature, $A = \pi \cdot d \cdot b$ is the tube cross-sectional area and $b = 0.34$ nm the tube wall thickness. The average tube temperature is used to compute the various $mfps$, and then $R(V,T)$ and I - V . The SWNT thermal conductivity is expected to follow $\kappa(T) = \kappa_0(T_0/T)$ at high temperatures due to Umklapp phonon-phonon scattering¹¹⁻¹² where κ_0 is the R. T. thermal conductivity. Since $R(V,T)$ and $I(V)$ depend on T , which is in turn dependent on I and $\kappa(T)$, we use an overdamped iterative approach to compute I - V until T converges within 0.1 K for each bias V .

If the optical phonon population is assumed in equilibrium with the lattice (acoustic phonon) temperature, the model (with $\kappa_0 \sim 1800 \text{ Wm}^{-1}\text{K}^{-1}$) can reproduce the I - V curve of the $L \sim 3 \text{ }\mu\text{m}$ suspended SWNT only under a staggeringly high peak lattice temperature of $T > 1500 \text{ K}$ at $V \sim 1.5 \text{ V}$. This is contradicted by the fact that suspended SWNTs under such bias were never oxidized or lost connection upon exposure to air or a partial pressure of oxygen (the onset of oxidation is known to occur at $T \sim 800 \text{ K}$ ¹³) until $V > \sim 2\text{-}2.5 \text{ V}$. Without the nanotube at exceedingly high lattice temperatures, a rational mechanism underlying the low current and NDC characteristic of suspended SWNTs is the existence of non-equilibrium, hot optical phonons. Since only few of the numerous optical branches of a SWNT are involved in scattering electrons⁶ their density of states is relatively small. Their population will quickly build up in a suspended tube if the emitted optical phonons cannot immediately decay into other (lower energy or electrically inactive) modes (Fig. 2b inset) or into the contacts. This is consistent with the over-population of the radial-breathing optical mode of suspended SWNTs observed in recent low temperature tunneling experiments¹⁴ and with narrower Raman phonon line-widths for suspended SWNTs.¹⁵ Recent theory has also suggested non-equilibrium optical phonons may exist under high biases in SWNTs on substrates.¹⁶

We model the non-equilibrium optical phonons with an effective temperature $T_{op}^{eff} = T_{ac} + \alpha(T_{ac} - T_0)$. This linear relation can be written since Joule power is primarily dissipated to the OP modes (which is the case for high bias transport in SWNTs) and then decays into AC modes (Fig. 2b inset) and to the environment (T_0), as previously used for treating non-equilibrium phonons in GaAs and Ge.^{17,18,19} The non-equilibrium coefficient $\alpha > 0$ can be interpreted as the ratio of the thermal resistance of OP-AC decay to that of AC

conduction along the tube, to contacts at T_0 . The I - V curves were then calculated by $I = V/R(V, T_{op}^{eff}, T_{ac})$. We found that with $\kappa(T_{ac}) = \kappa_0 (T_0 / T_{ac})$ where the R.T. thermal conductivity $\kappa_0 \sim 3600 \text{ Wm}^{-1}\text{K}^{-1}$ (in line with that of multi-walled nanotubes²⁰) and $\alpha = 2.4$, our model reproduced the experimental I - V curves including NDC remarkably well over a wide range of suspended SWNT lengths and biases (Fig. 2a and Fig. 3a). The self-heating (T_{op}^{eff} and T_{ac}) of the suspended SWNTs were also calculated at various biases (Fig. 2b). Importantly, the $I \sim 1/V$ shape of the I - V curves in the NDC region is found to strongly reflect the temperature dependence of the thermal conductivity $\kappa(T) \sim 1/T$ that results from Umklapp phonon scattering at R.T. and above^{11,12} (electron contribution negligible²¹). Alternative models for the T -dependence of the thermal conductivity (e.g., $\kappa(T) \sim \text{constant}$, or $\kappa(T) \sim \text{linearly decreasing in } T$) cannot reproduce the I - V characteristics of suspended SWNTs (Fig. 4a dashed lines). Thus, we show that self-heating and I - V measurements on suspended SWNTs can be exploited to probe their thermal conductivity from R.T. up to $\sim 700\text{K}$ (V up to $\sim 2.2 \text{ V}$).

Our study suggests that SWNTs suspended in vacuum, by virtue of their free unperturbed state, present the extreme scenario of longest optical phonon lifetime and hence the strongest non-equilibrium optical phonon population under current flow. The higher currents observed in nanotubes on substrates are owed to the substrate-tube interaction that aids heat dissipation and more importantly assists the relaxation of optical phonons emitted through electron scattering. Self-heating and hot phonons are also thought to exist in nanotubes lying on substrates,¹⁶ although at higher biases ($> \sim 1 \text{ V}$ in Fig. 2a) and electric fields than in suspended tubes. This raises the interesting possibility that SWNTs on substrates may be engineered to deliver currents significantly higher than previously

possible (for a given tube length) through rational interface design for optimized heat dissipation and optical phonon relaxation. This scenario is of considerable consequences for electronics and may have similar implications to high current application of quasi-1D materials in general. The effects uncovered here could also be exploited for new device applications of suspended SWNTs. For instance, we found that suspended semiconducting SWNTs exhibiting similar NDC under negative gate voltages lead to p-type nanotube field effect transistors (FET) with strong gate-dependent NDC in the on-state (Fig. 4b). These characteristics could lead to novel devices such as oscillators²² with gate-tunability.

We acknowledge valuable discussions with Ali Javey and Sanjiv Sinha. This work is supported by the MARCO MSD Focus Center.

References

1. Z. Yao, C. L. Kane, and C. Dekker, Phys. Rev. Lett. **84**, 2941 (2000).
2. A. Javey, P. Qi, Q. Wang, et al., Proc. Nat. Acad. Sci. **101**, 13408 (2004).
3. J. Cao, Q. Wang, D. Wang, et al., Small **1**, 138 (2005).
4. J. Cao, Q. Wang, M. Rolandi, et al., Phys. Rev. Lett. **93**, 216803 (2004).
5. G. Pennington and N. Goldsman, Phys. Rev. B **68**, 045426 (2003).
6. V. Perebeinos, J. Tersoff, and P. Avouris, Phys. Rev. Lett. **94**, 086802 (2005).
7. J. Y. Park, S. Rosenblatt, Y. Yaish, et al., Nano Letters **4**, 517 (2004).
8. S. Datta, *Electronic Transport in Mesoscopic Systems* (University Press, Cambridge, 1995).
9. A. Javey, J. Guo, M. Paulsson, et al., Phys. Rev. Lett. **92**, 106804 (2004).
10. D. Mann, A. Javey, J. Kong, et al., Nano Lett. **3**, 1541 (2003).
11. J. M. Ziman, *Electrons and Phonons* (Oxford Univ. Press, 1960).
12. M. A. Osman and D. Srivastava, Nanotechnology **12**, 21 (2001).
13. I. W. Chiang, B. E. Brinson, R. E. Smalley, et al., J. Phys. Chem. B **105**, 1157 (2001).
14. B. J. LeRoy, S. G. Lemay, J. Kong, et al., Nature **432**, 371 (2004).
15. H. Son, Y. Hori, S. G. Chou, et al., Appl. Phys. Lett. **85**, 4744 (2004).
16. M. Lazzeri, Piscanec, S., Mauri, et al., cond-mat/0503278 (2005).
17. S. Madhavi, V. Venkataraman, J. C. Sturm, et al., Phys. Rev. B **61**, 16807 (2000).
18. H. M. Van Driel, Phys. Rev. B **19**, 5928 (1979).
19. A. Majumdar, K. Fushinobu, and K. Hijikata, J. Appl. Phys. **77**, 6686 (1995).
20. P. Kim, L. Shi, A. Majumdar, et al., Phys. Rev. Lett. **87**, 215502/1 (2001).
21. T. Yamamoto, S. Watanabe, and K. Watanabe, Phys. Rev. Lett. **92**, 075502 (2004).
22. M. Shur, *Physics of Semiconducting Devices* (Prentice-Hall, 1990).

Figure Captions

Figure 1: Freely suspended nanotube devices. (a) Scanning electron microscope (SEM) image, taken at a 45° angle, of the non-suspended (on nitride) and suspended (over a $\sim 0.5 \mu\text{m}$ deep trench, entirety of trench depth not shown in the image) $L \sim 2 \mu\text{m}$ nanotube segments of an individual nanotube, both segments with Pt contacts under the tube.^{3,4} (b) A schematic of the device cross-section. (c) SEM image of a nanotube suspended over a trench across a $\sim 10 \mu\text{m}$ Pt electrode gap. The bright features between the Pt electrodes were metal lines at the bottom of the wide trench used as local gates. The diameters of the nanotubes were measured by AFM in the range of $d \sim 2\text{-}3 \text{ nm}$. Nanotubes grown under the same condition on transmission electron microscope (TEM) grids were confirmed to be single-walled by TEM.

Figure 2: High-field electron transport in suspended nanotubes. (a) Current-voltage (I - V) characteristics of the same-length ($L \sim 3 \mu\text{m}$) suspended and non-suspended portions of a SWNT ($d \sim 2.4 \text{ nm}$) at room temperature measured in vacuum. The symbols represent experimental data, the lines are calculations. (b) Computed average acoustic and effective optical phonon temperature vs. bias voltage for the suspended tube segment in (a) quantifying the degree of self-heating. The figure inset shows the energy flow in our model from electrons ('heated' by the electric-field) to optical phonons and then acoustic phonons. We estimated the heat dissipation by radiation (ignored in our model) to be less than 1 percent, even up to an average SWNT temperature $T = 900 \text{ K}$. Dissipation at the contacts ($I^2 R_c$) is estimated to be less than 5 percent.

Figure 3: Currents in various-length suspended SWNTs. (a) I - V of four suspended tubes with lengths: $L \sim 0.6, 2.1, 3$ and $11 \mu\text{m}$ respectively. Symbols are experimental data, solid lines are calculations. The tube diameters used in the calculation (consistent with AFM) were $d \sim 2, 2.4, 2.4$ and 3.2 nm respectively. The contact resistance R_c was used as a parameter to fit the I - V curves at low bias. $R_c \sim 15 \text{ k}\Omega$ for all tubes except for $L = 3 \mu\text{m}$ which had $R_c \sim 30 \text{ k}\Omega$. (b) Peak current for suspended SWNTs of various lengths. The error bars are based on tens of devices measured. The solid line is given by our theoretical model with $d = 2 \text{ nm}$ and assuming ideal contacts ($R_c = 0$). The peak current scales approximately as $\sim 1/L$ just like the thermal conductance of the suspended nanotubes, an additional indicator that this is a thermally-limited effect.

Figure 4: Thermal properties and potential novel devices. (a) I - V of a $2 \mu\text{m}$ suspended tube in vacuum (experimental data with symbols) and calculations (lines) based on three different thermal

conductivity $\kappa(T)$ models ($\kappa_0 = 3600 \text{ Wm}^{-1}\text{K}^{-1}$ and $T_0 \sim 300 \text{ K}$). The high bias region of the I - V curve provides an indirect measurement of the temperature dependence of the thermal conductivity for $T \gtrsim 400 \text{ K}$. (b) Measured I - V characteristics at various gate voltages (V_g) for a suspended semiconducting SWNT in FET geometry with the local gate at the bottom of the trench (see Fig. 1b). The inset plots the transfer characteristics, I - V_g curve recorded under a bias of $V \sim 1 \text{ mV}$.

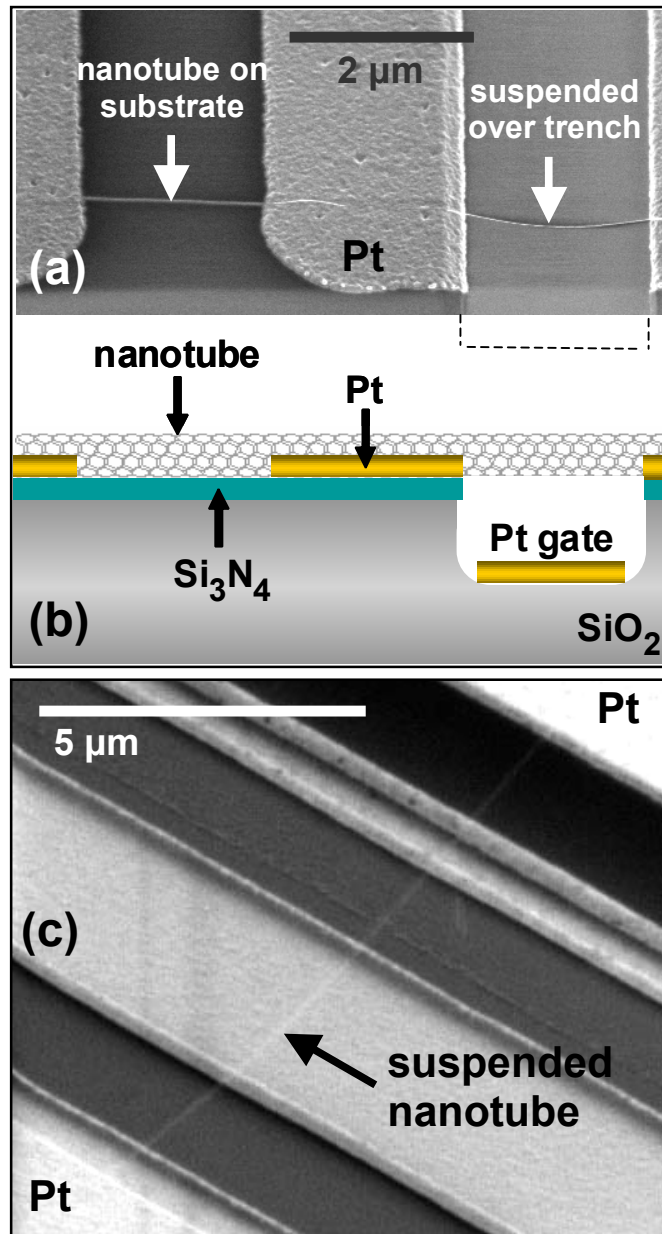


Figure 1.

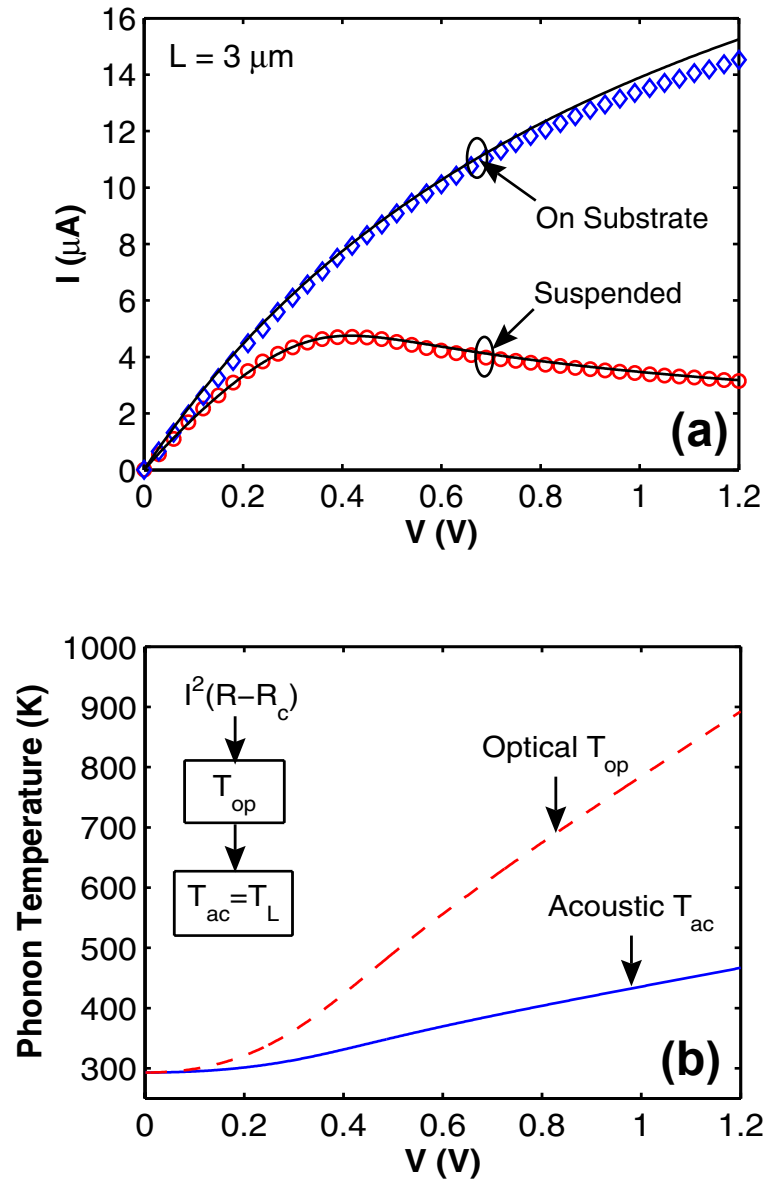


Figure 2.

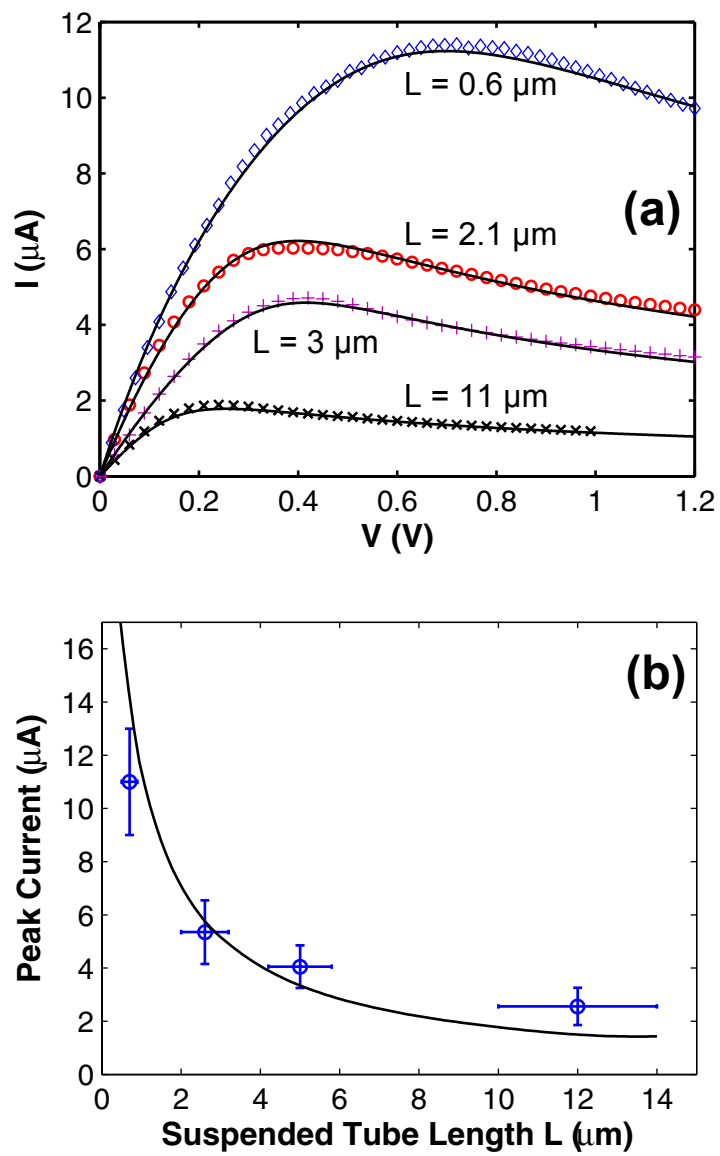


Figure 3.

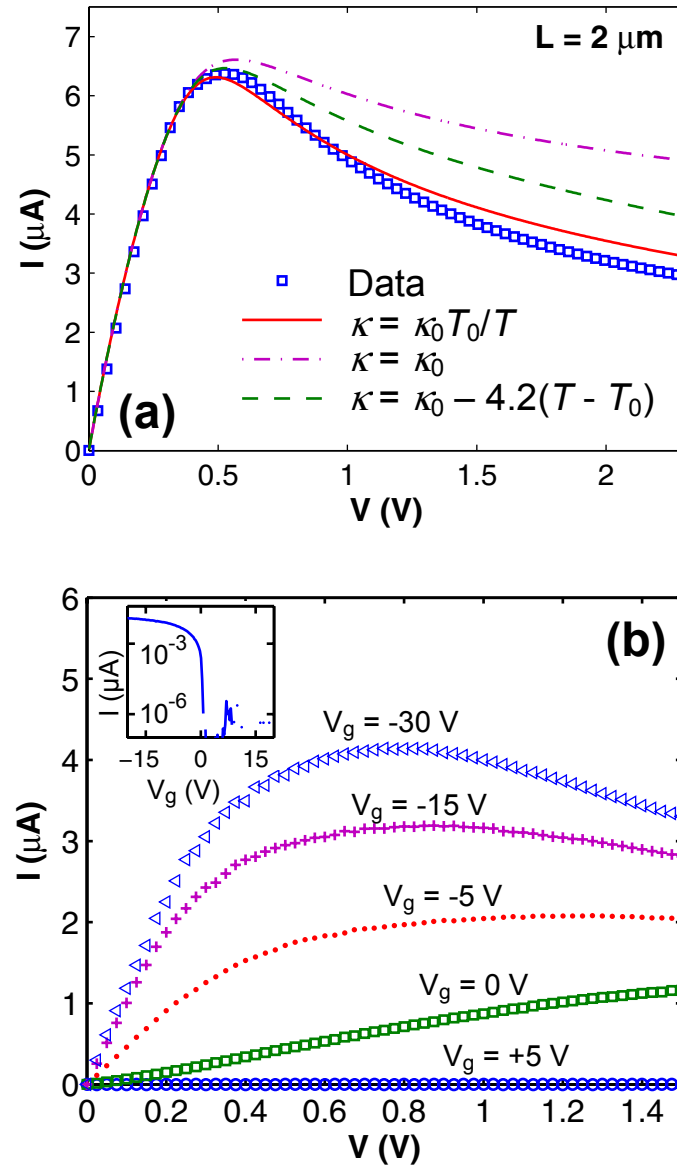


Figure 4.